Nuclear spin dependence of the reaction of H_3^+ with H_2. I. Kinetics and modeling

Kyle N. Crabtree,[1] Brian A. Tom,[1,a)] and Benjamin J. McCall[2,b)]
[1]*Department of Chemistry, University of Illinois, Urbana, Illinois 61801, USA*
[2]*Departments of Chemistry, Astronomy, and Physics, University of Illinois, Urbana, Illinois 61801, USA*

(Received 26 January 2011; accepted 17 April 2011; published online 19 May 2011)

The chemical reaction $H_3^+ + H_2 \rightarrow H_2 + H_3^+$ is the simplest bimolecular reaction involving a polyatomic, yet is complex enough that exact quantum mechanical calculations to adequately model its dynamics are still unfeasible. In particular, the branching fractions for the "identity," "proton hop," and "hydrogen exchange" reaction pathways are unknown, and to date, experimental measurements of this process have been limited. In this work, the nuclear-spin-dependent steady-state kinetics of the $H_3^+ + H_2$ reaction is examined in detail, and employed to generate models of the *ortho*:*para* ratio of H_3^+ formed in plasmas of varying *ortho*:*para* H_2 ratios. One model is based entirely on nuclear spin statistics, and is appropriate for temperatures high enough to populate a large number of H_3^+ rotational states. Efforts are made to include the influence of three-body collisions in this model by deriving nuclear spin product branching fractions for the $H_5^+ + H_2$ reaction. Another model, based on rate coefficients calculated using a microcanonical statistical approach, is appropriate for lower-temperature plasmas in which energetic considerations begin to compete with the nuclear spin branching fractions. These models serve as a theoretical framework for interpreting the results of laboratory studies on the reaction of H_3^+ with H_2. © *2011 American Institute of Physics*. [doi:10.1063/1.3587245]

I. INTRODUCTION

Symmetry and its associated selection rules have long been an integral component of spectroscopy.[1,2] For high-resolution spectroscopy, the complete nuclear permutation-inversion (CNPI) group representation[3–5] has been useful for assigning symmetry labels to rotational energy levels and calculating nuclear spin statistical weights (NSSWs), in particular for nonrigid molecules. The CNPI representation is based on the fact that the molecular Hamiltonian is invariant under permutations of identical nuclei and spatial inversion of all particles through the molecular center-of-mass, in contrast to point group theory, which depends on the geometrical symmetry of a set of nuclei.

The formulation of the CNPI groups allows for an easy determination of the consequences of Bose-Einstein (for integer-spin nuclei) or Fermi-Dirac (for half-integer-spin nuclei) statistics. According to Dirac's formulation[6] of the Pauli exclusion principle,[7] a molecular wavefunction must be symmetric with respect to permutation of identical bosons, and antisymmetric with respect to permutation of identical fermions. When applied to H_2 and H_3^+, the consequence is that the nuclear spin configuration of each molecule is linked to its rotational manifold. For H_2, the *ortho* configuration (o-H_2, $I = 1$) exists only in rotational levels in which J is odd, and the *para* configuration (p-H_2, $I = 0$) exists only in the even-J levels. The symmetry of H_3^+ is a bit more complex, but it can be shown that in the vibrational ground state, the nuclear spin configurations are linked to the projection quantum number k: o-$H_3^+(I = 3/2) \rightarrow k = 3n$, p-$H_3^+(I = 1/2) \rightarrow k = 3n \pm 1$, where n is an integer.[8]

Because the nuclear magnetic interaction is rather weak, the nuclear spin configurations of H_2 and H_3^+ behave as independent chemical species, meaning that I is a good quantum number in these systems. Interconversion between nuclear spin configurations in each of these molecules can only be accomplished by means of interaction with a strong, local, inhomogeneous magnetic field (such as the surface of a ferromagnetic catalyst), or by means of reactive collisions that result in scrambling of nuclei. The thermoneutral reaction $H_3^+ + H_2 \rightarrow H_2 + H_3^+$ is a prime example of this type of reaction. However, because I is a good quantum number in each molecule, this reaction is subject to selection rules[9,10] based on the conservation of the total nuclear spin of the system.

Beyond the fundamental interest of studying selection rules in chemical reactions, the reaction between H_3^+ and H_2 has practical application as well. Hydrogen is by far the most abundant element in the universe, and consequently H_2 and H_3^+ serve as useful probes of astrophysical or extraterrestrial conditions. In particular, H_3^+ has been used to image auroral activity in the atmospheres of Jupiter,[11] Saturn,[12] and Uranus ,[13] to probe gas density and temperature in the galactic center,[14] and to estimate the interstellar cosmic-ray ionization rate.[15,16] In molecular clouds, only the lowest states of o-H_3^+ and p-H_3^+ are populated, and the inferred *ortho*:*para* ratio of H_3^+ has been used to estimate interstellar cloud temperatures and dimensions.[15,17,18] In these environments, the $H_3^+ + H_2$ reaction is the dominant means by which the nuclear spin of

a)Present address: Department of Chemistry, United States Air Force Academy, Colorado 80840, USA.
b)Author to whom correspondence should be addressed. Electronic mail: bjmccall@illinois.edu.

H_3^+ can be changed, and the selection rules for this reaction have important implications for the use of H_3^+ as a temperature probe.[19]

To understand the $H_3^+ + H_2$ reaction, especially its role in the interstellar medium, laboratory measurements of its nuclear spin dependence are needed. Initial measurements of this reaction have been performed in a ~400 K hydrogenic plasma, but the associated analysis was rather complex, and not readily applicable to experiments at lower temperatures.[20] Furthermore, in a laboratory plasma, the gas density may be sufficiently high to allow for three-body reactions to occur. If these exhibit nuclear spin dependence, then they will interfere with the measurement of the two-body process. These effects were not taken into account in the previous work.

In this paper, we present chemical models aimed at assessing the nuclear spin dependence of the $H_3^+ + H_2$ reaction. The paper is structured as follows. In Sec. II, we examine in more detail the nuclear spin selection rules as they apply to reactions in laboratory plasmas. In Sec. III, we derive models for nuclear spin dependence in a laboratory plasma at high temperature, and then we derive a model for a low-temperature plasma in Sec. IV. We summarize the work in Sec. V. The models in this paper can be applied directly to experimental measurements, and are intended to serve as a framework for the interpretation of such measurements (see the following article in this issue[21]).

II. NUCLEAR SPIN SELECTION RULES

The nuclear spin selection rules[9,10] result in NSSWs for various nuclear spin reactant and product channels. If the energy available in a chemical reaction is sufficiently high, then these NSSWs describe the outcomes of the reaction in a statistical manner. We call this situation the "high temperature limit." The NSSWs have been derived for the $H_3^+ + H_2$ system by Oka[10] in terms of the rotation group representations of the nuclear spin angular momentum. For three-body collisions proceeding through a $(H_7^+)^*$ complex, the NSSWs for the seven-particle $H_5^+ + H_2$ system must be used. In this section, we review the NSSWs for the $H_3^+ + H_2$ system, and derive NSSWs for $H_5^+ + H_2$.

A. $H_3^+ + H_2$

The rotation group representation of the nuclear spin angular momentum of H_2 is $(\mathcal{D}_{1/2})^2 = \mathcal{D}_1 \oplus \mathcal{D}_0$, and that of H_3^+ is $(\mathcal{D}_{1/2})^3 = \mathcal{D}_{3/2} \oplus 2\mathcal{D}_{1/2}$. The correspondence between the representations and the nuclear spin states (with statistical weights in parentheses) is: $\mathcal{D}_1 \rightarrow o\text{-}H_2$ $(2 \times 1 + 1 = 3)$, $\mathcal{D}_0 \rightarrow p\text{-}H_2$ $(2 \times 0 + 1 = 1)$, $\mathcal{D}_{3/2} \rightarrow o\text{-}H_3^+$ $(2 \times 3/2 + 1 = 4)$, and $2\mathcal{D}_{1/2} \rightarrow p\text{-}H_3^+$ $(2[2 \times 1/2 + 1] = 4)$. Using the procedure described by Oka,[10] the NSSWs for the possible reactions between the nuclear spin configurations of H_3^+ and H_2 can be calculated, and these are shown for convenience in Table I.

In the $H_3^+ + H_2$ reaction, proton scrambling may be incomplete, as has been experimentally demonstrated for this system[20] and for the $D_3^+ + H_2$ system.[22] Following Oka, we

TABLE I. Total nuclear spin statistical weights for the $H_3^+ + H_2$ reaction (see Ref. 10). The table rows correspond to the nuclear spin configuration of reactant (H_3^+,H_2) pairs, and the table columns correspond to the product pairs.

(H_3^+,H_2)	Weight	$(\mathcal{D}_{3/2}, \mathcal{D}_1)$	$(\mathcal{D}_{3/2}, \mathcal{D}_0)$	$(\mathcal{D}_{1/2}, \mathcal{D}_1)$	$(\mathcal{D}_{1/2}, \mathcal{D}_0)$
$(\mathcal{D}_{3/2}, \mathcal{D}_1)$	12	37/5	1	14/5	4/5
$(\mathcal{D}_{3/2}, \mathcal{D}_0)$	4	1	1	2	0
$(\mathcal{D}_{1/2}, \mathcal{D}_1)$	12	14/5	2	28/5	8/5
$(\mathcal{D}_{1/2}, \mathcal{D}_0)$	4	4/5	0	8/5	8/5

define the three statistical reaction pathways as follows:

$$\tilde{H}_3^+ + H_2 \rightarrow \tilde{H}_3^+ + H_2, \tag{1}$$

$$\tilde{H}_3^+ + H_2 \rightarrow H_2\tilde{H}^+ + \tilde{H}_2, \tag{2}$$

$$\tilde{H}_3^+ + H_2 \rightarrow H\tilde{H}_2^+ + H\tilde{H}. \tag{3}$$

These are the identity (1), proton hop (2), and hydrogen exchange (3) pathways, with branching fractions S^{id}, S^{hop}, and S^{exch} (1/10, 3/10, and 6/10 in the statistical limit, respectively). NSSWs can be calculated for each of these individually, and the results organized in matrix form. The ordering of rows and columns in these matrices correspond to the ordering in Table I. The identity matrix is given by the statistical weight of each channel multiplied by S^{id}; the hop matrix is calculated by representing a proton hop as the sequence $H_3^+ \rightarrow H_2 + H^+$, followed by $H^+ + \tilde{H}_2 \rightarrow H\tilde{H}_2^+$ and applying Oka's method. Finally, the exchange matrix is obtained by subtracting the identity and hop matrices from the total matrix shown in Table I. These matrices are shown in Eqs. (4)–(6), along with their values in the statistical limit:

$$\text{id} = S^{id}\begin{pmatrix} 12 & 0 & 0 & 0 \\ 0 & 4 & 0 & 0 \\ 0 & 0 & 12 & 0 \\ 0 & 0 & 0 & 4 \end{pmatrix} \rightarrow \begin{pmatrix} 6/5 & 0 & 0 & 0 \\ 0 & 2/5 & 0 & 0 \\ 0 & 0 & 6/5 & 0 \\ 0 & 0 & 0 & 2/5 \end{pmatrix}, \tag{4}$$

$$\text{hop} = S^{hop}\begin{pmatrix} 8 & 0 & 4 & 0 \\ 0 & 0 & 4 & 0 \\ 4 & 4 & 2 & 2 \\ 0 & 0 & 2 & 2 \end{pmatrix} \rightarrow \begin{pmatrix} 12/5 & 0 & 6/5 & 0 \\ 0 & 0 & 6/5 & 0 \\ 6/5 & 6/5 & 3/5 & 3/5 \\ 0 & 0 & 3/5 & 3/5 \end{pmatrix}, \tag{5}$$

$$\text{exch} = S^{exch}\begin{pmatrix} 19/3 & 5/3 & 8/3 & 4/3 \\ 5/3 & 1 & 4/3 & 0 \\ 8/3 & 4/3 & 19/3 & 5/3 \\ 4/3 & 0 & 5/3 & 1 \end{pmatrix} \rightarrow \begin{pmatrix} 19/5 & 1 & 8/5 & 4/5 \\ 1 & 3/5 & 4/5 & 0 \\ 8/5 & 4/5 & 19/5 & 1 \\ 4/5 & 0 & 1 & 3/5 \end{pmatrix}. \tag{6}$$

TABLE II. Mechanism-specific nuclear spin branching fractions for the formation of *o*-H_3^+ and *p*-H_3^+ from the $H_3^+ + H_2$ reaction with the (H_3^+,H_2) reactant nuclear spin configurations.

	Hop		Exchange	
(H_3^+,H_2)	*o*-H_3^+	*p*-H_3^+	*o*-H_3^+	*p*-H_3^+
($\mathcal{D}_{3/2}$, $\mathcal{D}_1$)	2/3	1/3	2/3	1/3
($\mathcal{D}_{3/2}$, $\mathcal{D}_0$)	0	1	2/3	1/3
($\mathcal{D}_{1/2}$, $\mathcal{D}_1$)	2/3	1/3	1/3	2/3
($\mathcal{D}_{1/2}$, $\mathcal{D}_0$)	0	1	1/3	2/3

It is often the case that H_2 is more abundant than H_3^+ by several orders of magnitude, such as in a laboratory plasma, and therefore the nuclear spin configuration of the product H_2 might not be important, especially if the plasma is pulsed. The number of $H_3^+ + H_2$ collisions will not be sufficient to significantly change the H_2 *ortho*:*para* ratio, so the branching fractions for the formation of *o*-H_3^+ and *p*-H_3^+ can be calculated ignoring the nuclear spin of the product H_2. This can be done separately for the hop and exchange reactions, and the results are summarized in Table II.

B. $H_5^+ + H_2$

In a laboratory plasma, the collision rate may be high enough that during the lifetime of the $(H_5^+)^*$ complex formed by H_3^+ and H_2, the complex undergoes an additional collision with H_2. In such a three-body process, the excess energy of the complex may be drawn away, forming a stable H_5^+ species. Alternatively, the incoming H_2 may add to form an $(H_7^+)^*$ complex, where additional proton scrambling may occur, followed by the dissociation pathway $(H_7^+)^* \rightarrow (H_5^+)^* + H_2 \rightarrow H_3^+ + 2H_2$. To model this process, we must derive the NSSWs for the $H_5^+ + H_2$ system.

Following Oka's procedure, we first define the angular momentum representation of this reaction. H_5^+ is represented as $(\mathcal{D}_{1/2})^5 = \mathcal{D}_{5/2} \oplus 4\mathcal{D}_{3/2} \oplus 5\mathcal{D}_{1/2}$, and the reaction is represented by

$$\begin{aligned}&(\mathcal{D}_{5/2} \oplus 4\mathcal{D}_{3/2} \oplus 5\mathcal{D}_{1/2}) \otimes (\mathcal{D}_1 \oplus \mathcal{D}_0)\\ &\quad\rightarrow \mathcal{D}_{7/2} \oplus 6\mathcal{D}_{5/2} \oplus 14\mathcal{D}_{3/2} \oplus 14\mathcal{D}_{1/2}\\ &\quad\rightarrow (\mathcal{D}_{5/2} \oplus 4\mathcal{D}_{3/2} \oplus 5\mathcal{D}_{1/2}) \otimes (\mathcal{D}_1 \oplus \mathcal{D}_0).\end{aligned}$$

The reaction is then broken down into individual reactants. For this reaction, the forward and reverse reactions are identical, but to remain consistent with Oka's notation, the reverse reactions are

$$\begin{aligned}\mathcal{D}_{7/2} \oplus \mathcal{D}_{5/2} \oplus \mathcal{D}_{3/2} &\leftarrow \mathcal{D}_{5/2} \otimes \mathcal{D}_1,\\ \mathcal{D}_{5/2} &\leftarrow \mathcal{D}_{5/2} \otimes \mathcal{D}_0,\\ 4\mathcal{D}_{5/2} \oplus 4\mathcal{D}_{3/2} \oplus 4\mathcal{D}_{1/2} &\leftarrow 4\mathcal{D}_{3/2} \otimes \mathcal{D}_1,\\ 4\mathcal{D}_{3/2} &\leftarrow 4\mathcal{D}_{3/2} \otimes \mathcal{D}_0,\\ 5\mathcal{D}_{3/2} \oplus 5\mathcal{D}_{1/2} &\leftarrow 5\mathcal{D}_{1/2} \otimes \mathcal{D}_1,\\ 5\mathcal{D}_{1/2} &\leftarrow 5\mathcal{D}_{1/2} \otimes \mathcal{D}_0.\end{aligned}$$

This leads to the normalized outcomes for the intermediates:

$$\begin{aligned}\mathcal{D}_{7/2} &\rightarrow 8(\mathcal{D}_{5/2} \otimes \mathcal{D}_1/18),\\ \mathcal{D}_{5/2} &\rightarrow (\mathcal{D}_{5/2} \otimes \mathcal{D}_1/18) \oplus (\mathcal{D}_{5/2} \otimes \mathcal{D}_0/6)\\ &\quad \oplus 4(\mathcal{D}_{3/2} \otimes \mathcal{D}_1/12),\\ \mathcal{D}_{3/2} &\rightarrow \frac{2}{7}(\mathcal{D}_{5/2} \otimes \mathcal{D}_1/18) \oplus \frac{8}{7}(\mathcal{D}_{3/2} \otimes \mathcal{D}_1/12)\\ &\quad \oplus \frac{8}{7}(\mathcal{D}_{3/2} \otimes \mathcal{D}_0/4) \oplus \frac{10}{7}(\mathcal{D}_{1/2} \otimes \mathcal{D}_1/6),\\ \mathcal{D}_{1/2} &\rightarrow \frac{4}{7}(\mathcal{D}_{3/2} \otimes \mathcal{D}_1/12) \oplus \frac{5}{7}(\mathcal{D}_{1/2} \otimes \mathcal{D}_1/6)\\ &\quad \oplus \frac{5}{7}(\mathcal{D}_{1/2} \otimes \mathcal{D}_0/2).\end{aligned}$$

From here, the calculation of the total NSSW matrix is possible, and an example will be given for completeness. To calculate a NSSW, the total weights of possible reaction pathways for a given reactant-product pair must be added. For reactant pair ($\mathcal{D}_{3/2}$, $\mathcal{D}_1$) and product pair ($\mathcal{D}_{5/2}$, $\mathcal{D}_1$), this proceeds as follows: the reactant $4(\mathcal{D}_{3/2} \otimes \mathcal{D}_1)$ gives the intermediates $4\mathcal{D}_{5/2}$, $4\mathcal{D}_{3/2}$, and $4\mathcal{D}_{1/2}$. For each intermediate, the normalized weight corresponding to the product $(\mathcal{D}_{5/2} \otimes \mathcal{D}_1)$ is its coefficient in the appropriate normalized outcome listed above. For the $4\mathcal{D}_{1/2}$ intermediates, the desired product is not obtained; for the $4\mathcal{D}_{5/2}$ and $4\mathcal{D}_{3/2}$ intermediates, the coefficients are 4×1 and $4 \times 2/7$, respectively, giving a total weight of 36/7. The reverse reaction ($\mathcal{D}_{5/2}$, $\mathcal{D}_1$) $\rightarrow$ ($\mathcal{D}_{3/2}$, $\mathcal{D}_1$) has the same weight, as the reaction is symmetric. The NSSWs for all reactant and product pairs are listed in Table III.

To calculate mechanism-specific NSSWs, the next step is to define the statistical mechanisms for the system:

$$H_5^+ + \tilde{H}_2 \rightarrow H_5^+ + \tilde{H}_2, \tag{7}$$

$$H_5^+ + \tilde{H}_2 \rightarrow H_3\tilde{H}_2^+ + H_2, \tag{8}$$

TABLE III. As Table I, for the $H_5^+ + H_2$ reaction.

(H_5^+,H_2)	Weight	($\mathcal{D}_{5/2}$, $\mathcal{D}_1$)	($\mathcal{D}_{5/2}$, $\mathcal{D}_0$)	($\mathcal{D}_{3/2}$, $\mathcal{D}_1$)	($\mathcal{D}_{3/2}$, $\mathcal{D}_0$)	($\mathcal{D}_{1/2}$, $\mathcal{D}_1$)	($\mathcal{D}_{1/2}$, $\mathcal{D}_0$)
($\mathcal{D}_{5/2}$, $\mathcal{D}_1$)	18	65/7	1	36/7	8/7	10/7	0
($\mathcal{D}_{5/2}$, $\mathcal{D}_0$)	6	1	1	4	0	0	0
($\mathcal{D}_{3/2}$, $\mathcal{D}_1$)	48	36/7	4	160/7	32/7	60/7	20/7
($\mathcal{D}_{3/2}$, $\mathcal{D}_0$)	16	8/7	0	32/7	32/7	40/7	0
($\mathcal{D}_{1/2}$, $\mathcal{D}_1$)	30	10/7	0	60/7	40/7	75/7	25/7
($\mathcal{D}_{1/2}$, $\mathcal{D}_0$)	10	0	0	20/7	0	25/7	25/7

TABLE IV. Values of g_{pI} for product pair p and intermediate angular momentum representation $\mathcal{D}_I$.

p	$\mathcal{D}_{7/2}$	$\mathcal{D}_{5/2}$	$\mathcal{D}_{3/2}$	$\mathcal{D}_{1/2}$
$(\mathcal{D}_{5/2}, \mathcal{D}_1)$	8	6	4	0
$(\mathcal{D}_{5/2}, \mathcal{D}_0)$	0	6	0	0
$(\mathcal{D}_{3/2}, \mathcal{D}_1)$	0	6	4	2
$(\mathcal{D}_{3/2}, \mathcal{D}_0)$	0	0	4	0
$(\mathcal{D}_{1/2}, \mathcal{D}_1)$	0	0	4	2
$(\mathcal{D}_{1/2}, \mathcal{D}_0)$	0	0	0	2

$$H_5^+ + \tilde{H}_2 \rightarrow H_4\tilde{H}^+ + \tilde{H}H. \tag{9}$$

Reaction (7) is the "identity" mechanism with statistical weight 1, (8) is the "H_3^+ hop" mechanism with statistical weight 10, and (9) is the "hydrogen exchange" mechanism with statistical weight 10. However, both the H_3^+ hop and hydrogen exchange pathways are complex, and application of Oka's method for calculating mechanism-specific NSSWs is nontrivial.

An alternative formulation for calculating the NSSWs of the $H_3^+ + H_2$ system has been demonstrated by Park and Light,[23] and this approach can be more readily applied to the $H_5^+ + H_2$ system. Using the statistical mechanisms (7), (8), and (9), the mechanism-specific NSSW (B_{pr}^M) for reactant pair r and product pair p through mechanism M can be calculated by

$$B_{pr}^M = S^M \sum_I g_{pI} P_{pIr}^M, \tag{10}$$

where g_{pI} is the statistical weight of the $\mathcal{D}_I$ representation leading to p, S^M is the statistical weight of the reaction pathway, and P_{pIr}^M is the cumulative spin modification probability for reactant r to product p through an intermediate with angular momentum I. The values of g_{pI} can be found in Table IV. In the statistical limit, S^{id} is 1/21, and S^{hop} and S^{exch} are 10/21.

Calculation of P_{pIr}^M requires construction of basis states for calculating transition matrix elements. The easiest basis set for defining the scrambling operators is that of proton nuclear spin angular momentum projections. This basis set is defined by the projection quantum number of the nuclear spin angular momentum of each proton in the $(H_aH_bH_cH_dH_e)^+ + (H_fH_g)$ system: $|m_a, m_b, m_c, m_d, m_e, m_f, m_g\rangle$ (as a general note on notation, m represents a projection quantum number, and I represents a total angular momentum quantum number). In this basis set, the scrambling operators take very simple forms: $O^{\text{id}} = \hat{I}$, $O^{\text{hop}} = \hat{p}_{af}\hat{p}_{bg}$, and $O^{\text{exch}} = \hat{p}_{ef}$, where $\hat{p}_{ab}$ is a permutation operator for nuclei a and b.

TABLE V. Angular momentum substates for each I_5 state of H_5^+.

I_5	Substates (I_3, I_{ab}, I_{de})
5/2	(3/2,1,1)
3/2	(3/2,1,1), (3/2,1,0), (1/2,1,1), (1/2,0,1)
1/2	(3/2,1,1), (1/2,1,1), (1/2,0,1), (1/2,1,0), (1/2,0,0)

However, these 128 (2^7) orthonormal basis states do not directly map to the 128 reactant/product pair states, which are $18 \times (\mathcal{D}_{5/2}, \mathcal{D}_1)$, $6 \times (\mathcal{D}_{5/2}, \mathcal{D}_0)$, $12 \times 4(\mathcal{D}_{3/2}, \mathcal{D}_1)$, $4 \times 4(\mathcal{D}_{3/2}, \mathcal{D}_0)$, $6 \times 5(\mathcal{D}_{1/2}, \mathcal{D}_1)$, and $2 \times 5(\mathcal{D}_{1/2}, \mathcal{D}_0)$. Instead, these states are represented by the orthonormal total nuclear spin basis states $|I_7, m_7, I_5, I_3, I_{ab}, I_{de}, I_2\rangle$. In this form, I_5 and I_2 are the total nuclear spin angular momenta of H_5^+ and H_2, and I_7 and m_7 are the total nuclear spin angular momentum of the entire system and its projection. The quantities I_{ab} and I_{de} are the combined nuclear spin angular momenta of the (a, b) and (d, e) proton pairs in H_5^+, and I_3 is the combined angular momentum of I_{ab} and I_c. Together, I_3, I_{ab}, and I_{de} specify angular momentum substates of the I_5 state of H_5^+ (see Table V). The elements of these substates can be compared to the elements of the basis states of Park and Light for the $H_3^+ + H_2$ system (our notation is slightly different): $I_5 \rightarrow I$, $m_5 \rightarrow I_z$, $I_3 \rightarrow I_3$, $I_{ab} \rightarrow i_2$, and $I_{de} \rightarrow I_2$.

The orthonormal nuclear spin angular momentum basis states $|I_7, m_7, I_5, I_3, I_{ab}, I_{de}, I_2\rangle$ can be constructed from linear combinations of the proton projection basis states $|m_a, m_b, m_c, m_d, m_e, m_f, m_g\rangle$; the weighting coefficients are products of Clebsch-Gordan coefficients as shown in Eq. (11). The projections are defined explicitly as follows: $m_2 = m_f + m_g$, $m_{ab} = m_a + m_b$, $m_{de} = m_d + m_e$, $m_3 = m_{ab} + m_c$, and $m_5 = m_3 + m_{de}$.

$$\begin{aligned}|I_7, m_7, I_5, I_3, I_{ab}, I_{de}, I_2\rangle = \sum_{m_a,m_b,m_c,m_d,m_e,m_f,m_g} & \langle I_5, m_5; I_2, m_2 | I_7, m_7\rangle \langle I_3, m_3; I_{de}, m_{de} | I_5, m_5\rangle \\ & \times \langle I_{ab}, m_{ab}; I_c, m_c |\, I_3, m_3\rangle \langle I_d, m_d; I_e, m_e |\, I_{de}, m_{de}\rangle \langle I_a, m_a; I_b, m_b |\, I_{ab}, m_{ab}\rangle \\ & \times \langle I_f, m_f; I_g, m_g | I_2, m_2\rangle |m_a, m_b, m_c, m_d, m_e, m_f, m_g\rangle,\end{aligned} \tag{11}$$

Having defined the orthonormal total nuclear spin angular momentum basis states and the linear combinations of proton basis states that compose them, the mechanism-specific cumulative nuclear spin modification probability P_{pIr}^M can be calculated [Eq. (12)]. The summation takes into account the factors of 4 and 5 for $\mathcal{D}_{3/2}$ and $\mathcal{D}_{1/2}$ as seen in the rotation group representation of H_5^+ ($\mathcal{D}_{5/2} \oplus 4\mathcal{D}_{3/2} \oplus 5\mathcal{D}_{1/2}$). All values of P_{pIr}^M are shown in Table VI.

$$P_{pIr}^M = \sum_{I_3^p, I_{ab}^p, I_{de}^p, I_3^r, I_{ab}^r, I_{de}^r} \left| \left\langle I_7, m_7, I_5^p, I_3^p, I_{ab}^p, I_{de}^p, I_2^p \right| O^M \left| I_7, m_7, I_5^r, I_3^r, I_{ab}^r, I_{de}^r, I_2^r \right\rangle \right|^2, \tag{12}$$

Using the P_{pIr}^M values in Table VI with Eq. (10) allows calculation of the mechanism-specific NSSWs. Equations (13)–(15) show the branching fraction matrices as a function of S^M, and also show the matrices in the statistical limit ($S^{\text{id}} = 1/21$, $S^{\text{hop}} = 10/21$, and $S^{\text{exch}} = 10/21$). These matrices are ordered the same as Table III.

$$\text{id} = S^{\text{id}} \begin{pmatrix} 18 & 0 & 0 & 0 & 0 & 0 \\ 0 & 6 & 0 & 0 & 0 & 0 \\ 0 & 0 & 48 & 0 & 0 & 0 \\ 0 & 0 & 0 & 16 & 0 & 0 \\ 0 & 0 & 0 & 0 & 30 & 0 \\ 0 & 0 & 0 & 0 & 0 & 10 \end{pmatrix}$$

$$\rightarrow \begin{pmatrix} 6/7 & 0 & 0 & 0 & 0 & 0 \\ 0 & 2/7 & 0 & 0 & 0 & 0 \\ 0 & 0 & 16/7 & 0 & 0 & 0 \\ 0 & 0 & 0 & 16/21 & 0 & 0 \\ 0 & 0 & 0 & 0 & 10/7 & 0 \\ 0 & 0 & 0 & 0 & 0 & 10/21 \end{pmatrix}, \quad (13)$$

$$\text{hop} = S^{\text{hop}} \begin{pmatrix} 9 & 0 & 6 & 0 & 3 & 0 \\ 0 & 0 & 6 & 0 & 0 & 0 \\ 6 & 6 & 20 & 4 & 10 & 2 \\ 0 & 0 & 4 & 4 & 8 & 0 \\ 3 & 0 & 10 & 8 & 5 & 4 \\ 0 & 0 & 2 & 0 & 4 & 4 \end{pmatrix}$$

$$\rightarrow \begin{pmatrix} 30/7 & 0 & 20/7 & 0 & 10/7 & 0 \\ 0 & 0 & 20/7 & 0 & 0 & 0 \\ 20/7 & 20/7 & 200/21 & 40/21 & 100/21 & 20/21 \\ 0 & 0 & 40/21 & 40/21 & 80/21 & 0 \\ 10/7 & 0 & 100/21 & 80/21 & 50/21 & 40/21 \\ 0 & 0 & 20/21 & 0 & 40/21 & 40/21 \end{pmatrix}, \quad (14)$$

$$\text{exch} = S^{\text{exch}} \begin{pmatrix} 87/10 & 21/10 & 24/5 & 12/5 & 0 & 0 \\ 21/10 & 3/2 & 12/5 & 0 & 0 & 0 \\ 24/5 & 12/5 & 116/5 & 28/5 & 8 & 4 \\ 12/5 & 0 & 28/5 & 4 & 4 & 0 \\ 0 & 0 & 8 & 4 & 29/2 & 7/2 \\ 0 & 0 & 4 & 0 & 7/2 & 5/2 \end{pmatrix}$$

$$\rightarrow \begin{pmatrix} 29/7 & 1 & 16/7 & 8/7 & 0 & 0 \\ 1 & 5/7 & 8/7 & 0 & 0 & 0 \\ 16/7 & 8/7 & 232/21 & 56/21 & 80/21 & 40/21 \\ 8/7 & 0 & 56/21 & 40/21 & 40/21 & 0 \\ 0 & 0 & 80/21 & 40/21 & 145/21 & 35/21 \\ 0 & 0 & 40/21 & 0 & 35/21 & 25/21 \end{pmatrix}. \quad (15)$$

Adding the statistical matrices for the identity, H_3^+ hop, and hydrogen exchange mechanisms gives the total NSSW matrix:

$$\begin{pmatrix} 65/7 & 1 & 36/7 & 8/7 & 10/7 & 0 \\ 1 & 1 & 4 & 0 & 0 & 0 \\ 36/7 & 4 & 160/7 & 32/7 & 60/7 & 20/7 \\ 8/7 & 0 & 32/7 & 32/7 & 40/7 & 0 \\ 10/7 & 0 & 60/7 & 40/7 & 75/7 & 25/7 \\ 0 & 0 & 20/7 & 0 & 25/7 & 25/7 \end{pmatrix}.$$

These are identical to the total NSSWs calculated using Oka's method (Table III), which suggests that the calculation has been done properly. As with the $H_3^+ + H_2$ reaction, in a pulsed laboratory plasma the spin configuration of the product H_2 is not important, and the mechanism-specific branching fractions can be further reduced in terms of the branching fractions for the $\mathcal{D}_{5/2}$, $\mathcal{D}_{3/2}$, and $\mathcal{D}_{1/2}$ spin configurations of H_5^+. These results are in Table VII.

III. HIGH TEMPERATURE MODEL

At sufficiently high temperature, the NSSWs calculated in Sec. II can be exploited to determine the outcome of a large number of $H_3^+ + H_2$ collisions. In this section, we derive a model for the resultant p-H_3^+ fraction (p_3) at steady state in a plasma of a certain p-H_2 fraction (p_2), considering only two-body H_3^+-H_2 collisions. We then derive a model that takes into account the possibility of three-body collisions.

A. Two-body high temperature model

In a laboratory plasma consisting only of hydrogen, the chemistry occurring is relatively simple compared to other plasmas. H_2 is ionized by electron impact to give predominantly H_2^+. H_2^+ is destroyed very rapidly by the reaction $H_2^+ + H_2 \rightarrow H_3^+ + H$, causing H_3^+ to typically be the dominant ion in the plasma.[24,25] H_3^+ can undergo proton scrambling reactions with H_2, and can form larger H_{2n+1}^+ clusters through three-body reactions. H_3^+ and larger clusters are all destroyed either by further cluster formation, dissociative recombination, or ambipolar diffusion. Finally, hydrogen atoms can recombine in a three-body process to re-form H_2.

To study the $H_3^+ + H_2$ reaction, it is desirable to isolate the process as much as possible, which can be accomplished by tuning plasma conditions. If the *ortho*:*para* ratio of H_3^+ is established primarily by this reaction, as opposed to any other nuclear-spin-dependent processes, then the nuclear spin dependence can be directly inferred. Because H_3^+ formation[10] and destruction via dissociative recombination with electrons[26–28] exhibit spin dependence, the $H_3^+ + H_2$ reaction can control the *ortho*:*para* ratio of H_3^+ only if H_3^+ undergoes many collisions with H_2 prior to its destruction.

However, a more subtle effect is the H atom recombination to form H_2. The *ortho*:*para* ratio of H_2 in the plasma is equally as important as that of H_3^+. For instance, in a plasma of pure p-H_2 at room temperature, the H atom recombination on the walls of the containment vessel will produce normal-H_2 (n-H_2: 25% p-H_2, 75% o-H_2). Over time, this will cause a reduction in the p-H_2 fraction. This effect is in addition to the change in p-H_2 fraction caused by the $H_3^+ + H_2$ reaction itself.

TABLE VI. Mechanism-specific cumulative nuclear spin modification probabilities P^M_{pIr} for $H_5^+ + H_2$.

Reactant	Total spin	Mechanism	Product p					
r	I	M	(5/2,1)	(5/2,0)	(3/2,1)	(3/2,0)	(1/2,1)	(1/2,0)
		id	1	0	0	0	0	0
	7/2	hop	1	0	0	0	0	0
		exch	1	0	0	0	0	0
		id	1	0	0	0	0	0
(5/2,1)	5/2	hop	4/25	0	21/25	0	0	0
		exch	9/100	35/100	56/100	0	0	0
		id	1	0	0	0	0	0
	3/2	hop	1/100	0	24/100	0	75/100	0
		exch	1/25	0	9/25	15/25	0	0
		id	0	1	0	0	0	0
(5/2,0)	5/2	hop	0	0	1	0	0	0
		exch	7/20	5/20	8/20	0	0	0
		id	0	0	4	0	0	0
	5/2	hop	21/25	25/25	54/25	0	0	0
		exch	14/25	10/25	76/25	0	0	0
		id	0	0	4	0	0	0
(3/2,1)	3/2	hop	18/75	0	107/75	75/75	100/75	0
		exch	27/75	0	43/75	105/75	125/75	0
		id	0	0	4	0	0	0
	1/2	hop	0	0	2/3	0	7/3	3/3
		exch	0	0	4/3	0	2/3	6/3
		id	0	0	0	4	0	0
(1/2, 0)	3/2	hop	0	0	1	1	2	0
		exch	3/5	0	7/5	5/5	5/5	0
		id	0	0	0	0	5	0
	3/2	hop	9/12	0	16/12	24/12	11/12	0
		exch	0	0	5/3	3/3	7/3	0
(1/2,1)								
		id	0	0	0	0	5	0
	1/2	hop	0	0	7/3	0	2/3	6/3
		exch	0	0	2/3	0	31/12	7/4
		id	0	0	0	0	0	5
(1/2,0)	1/2	hop	0	0	1	0	2	2
		exch	0	0	8/4	0	7/4	5/4

An additional constraint, therefore, is that the plasma should be pulsed, and measurements taken as soon as possible after steady state is reached to avoid changes in the p-H_2 fraction. These conditions could be met in a pulsed hollow cathode discharge, or alternatively by storing H_3^+ in a radiofrequency ion trap with H_2 as a buffer gas.

Provided sufficient H_3^+-H_2 collisions occur, the *ortho*:*para* H_3^+ ratio can be modeled using the nuclear spin branching fractions from Table II. To begin, we model $d/dt([p\text{-}H_3^+])$ in terms of the hop and exchange reactions involving all combinations of o-H_3^+, p-H_3^+, o-H_2, and p-H_2 (square brackets, such as $[p\text{-}H_3^+]$, denote number

TABLE VII. Fractional H_5^+ spin product outcomes of the $H_5^+ + H_2$ reaction.

	Hop			Exchange		
Reactant pair	$\mathcal{D}_{5/2}$	$\mathcal{D}_{3/2}$	$\mathcal{D}_{1/2}$	$\mathcal{D}_{5/2}$	$\mathcal{D}_{3/2}$	$\mathcal{D}_{1/2}$
$(\mathcal{D}_{5/2}, \mathcal{D}_1)$	3/6	2/6	1/6	3/5	2/5	0
$(\mathcal{D}_{5/2}, \mathcal{D}_0)$	0	1	0	3/5	2/5	0
$(\mathcal{D}_{3/2}, \mathcal{D}_1)$	1/4	2/4	1/4	3/20	12/20	5/20
$(\mathcal{D}_{3/2}, \mathcal{D}_0)$	0	1/2	1/2	3/20	12/20	5/20
$(\mathcal{D}_{1/2}, \mathcal{D}_1)$	1/10	6/10	3/10	0	2/5	3/5
$(\mathcal{D}_{1/2}, \mathcal{D}_0)$	0	1/5	4/5	0	2/5	3/5

densities):

$$\frac{d[p\text{-}H_3^+]}{dt} = \left\{k^H\left(\frac{1}{3}[o\text{-}H_2] + 1[p\text{-}H_2]\right) + k^E\left(\frac{1}{3}[o\text{-}H_2] + \frac{1}{3}[p\text{-}H_2]\right)\right\}[o\text{-}H_3^+] - \left\{k^H\left(\frac{2}{3}[o\text{-}H_2] + 0[p\text{-}H_2]\right) + k^E\left(\frac{1}{3}[o\text{-}H_2] + \frac{1}{3}[p\text{-}H_2]\right)\right\}[p\text{-}H_3^+], \quad (16)$$

where k^H and k^E are the rates of the proton hop and hydrogen exchange reactions. The choice of using $d/dt([p\text{-}H_3^+])$ is arbitrary; the final result is the same if $d/dt([o\text{-}H_3^+])$ is used instead as a starting point. Invoking the steady state approximation, this equation is equal to 0.

Rather than working with absolute number densities, it is more convenient to work with spin state fractions. Because $[p\text{-}H_3^+] + [o\text{-}H_3^+] = [H_3^+]$ (and likewise for $[H_2]$), the number densities of the spin states can be expressed by a single parameter; in this case we choose the *para*-fractions $p_3 \equiv [p\text{-}H_3^+]/[H_3^+]$ and $p_2 \equiv [p\text{-}H_2]/[H_2]$. Dividing the equation by the product $[H_3^+][H_2]$ gives

$$0 = \left\{k^H\left(\frac{1}{3}(1-p_2) + p_2\right) + k^E\left(\frac{1}{3}(1-p_2) + \frac{1}{3}p_2\right)\right\}(1-p_3) - \left\{k^H\left(\frac{2}{3}(1-p_2)\right) + k^E\left(\frac{1}{3}(1-p_2) + \frac{1}{3}p_2\right)\right\}p_3.$$

This can be solved for p_3 and simplified:

$$p_3 = \frac{k^H\left(\frac{1}{3} + \frac{2}{3}p_2\right) + \frac{1}{3}k^E}{k^H + \frac{2}{3}k^E}.$$

The quantity $k^E/3$ can be factored from both the numerator and denominator. Defining $\alpha \equiv k^H/k^E = S^{hop}/S^{exch}$ gives the final result:

$$p_3 = \frac{\alpha + 2\alpha p_2 + 1}{3\alpha + 2}. \quad (17)$$

Equation (17) is a remarkably simple expression that allows for an experimental determination of the hop-to-exchange ratio α by measuring p_3 in a plasma of known p_2. As seen in Fig. 1, this model suggests that the relationship between p_3 and p_2 is linear, and that the slope should be related to α. It also suggests that no matter the value of α, a n-H_2 plasma ($p_2 = 0.25$) should produce n-H_3^+ (50% *o*-H_3^+, 50% *p*-H_3^+). The most sensitive probe of α would be an experiment performed with pure *p*-H_2. This has been done by Cordonnier *et al.*[20], who found that in a ~400 K *p*-H_2 pulsed hollow cathode plasma, p_3 was 0.89 or 0.91, depending on which spectroscopic transitions were observed. Using Eq. (17), these give $\alpha = 2.4$ or 3.0, respectively, which are the same values they derived using a complex kinetic model including H_3^+ formation, dissociative recombination, and ambipolar diffusion. This gives some validation to the assumptions that went into the derivation of our simplified model.

An important question to consider is the timescale on which steady state is reached. Dividing Eq. (16) by $[H_3^+]$ and integrating gives

$$p_3(t) = p_{3,\infty} - (p_{3,\infty} - p_{3,o})\exp\left\{-\left(k^H + \frac{2}{3}k^E\right)[H_2]t\right\},$$

where $p_{3,\infty}$ and $p_{3,o}$ are the values of p_3 at $t = \infty$ and $t = 0$, respectively. The argument in the exponential is an expression nearly equal to the reactive collision rate of H_3^+ and H_2. After a few reactive collisions, p_3 should already be at its steady state value.

This model is valid only if p_2 is constant, which is the case if H_2 has an independent means of thermalizing its spin temperature at a constant value, or at early stages of a cw discharge before H atom recombination and proton scrambling can lead to significant changes in p_2. In a cw *p*-H_2 plasma at room temperature, this model can still be applied, but p_2 will have to be replaced by a function $p_2(t)$ to include the long-term time dependence of p_2. There may be cases in which the $H_3^+ + H_2$ reaction is the only means by which the spin of H_2 can be converted; in these cases it is possible to set up a pair of coupled differential equations that will give the steady state values of p_3 and p_2, but such a model is beyond the scope of this paper.

B. Three-body high temperature model

The model derived in the previous section ignores the possibility of any three-body processes occurring in the plasma. This assumption is valid so long as the pressure is sufficiently low, or if three-body reactions do not exhibit any appreciable nuclear spin dependence on H_3^+. If these conditions are not met, then values of α derived from interpretations of laboratory data based on the two-body model may be inaccurate. Through more detailed modeling, it may be possible to detect and disentangle any three-body processes from the underlying two-body process. There are two three-body reactions to consider: H_5^+ formation via $H_3^+ + 2H_2 \rightarrow H_5^+ + H_2$, and proton scrambling through a $(H_7^+)^*$ collision complex via $H_3^+ + 2H_2 \rightarrow (H_5^+)^* + H_2 \rightarrow (H_7^+)^* \rightarrow H_3^+ + 2H_2$.

The H_5^+ formation reaction has been studied by Paul *et al.*[29] by introducing H_3^+ into a 10 K radiofrequency ion trap surrounded by a bath of H_2 with a known *p*-H_2 fraction. They observed that H_5^+ formation was much more rapid when *p*-H_2

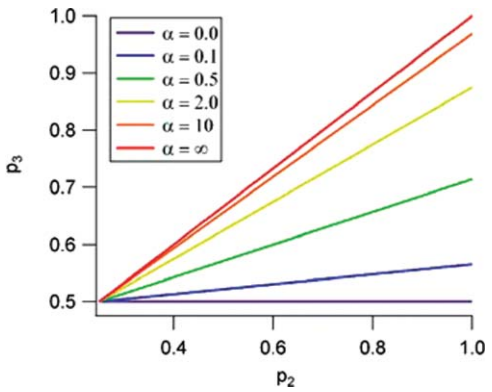

FIG. 1. The two-body high temperature model [Eq. (17)] for values of α ranging from 0 (purple, horizontal) to ∞ (red, steepest slope).

TABLE VIII. Reactions and rates used in the three-body high temperature model. The nuclear spin dependence of each reaction is not listed explicitly here. The final reaction is written so as to only allow for $(H_5^+)^*$ to undergo at most one collision with H_2. The superscript L refers to a Langevin rate coefficient, and the superscript u refers to a unimolecular dissociation rate coefficient.

Reaction	Rate
$H_3^+ + H_2 \rightarrow (H_5^+)^*$	$k_{3,2}^L[H_3^+][H_2]$
$(H_5^+)^* \rightarrow H_3^+ + H_2$	$k_5^u[(H_5^+)^*]$
$(H_5^+)^* + H_2 \rightarrow (H_7^+)^*$	$k_{5,2}^L[(H_5^+)^*][H_2]$
$(H_7^+)^* \rightarrow H_3^+ + 2H_2$	$k_7^u[(H_7^+)^*]$

was used instead of n-H_2. However, they did not investigate whether there was a dependence on the p-H_3^+ fraction; their experiments were performed with n-H_3^+. It is unknown whether the different nuclear spin configurations of the $(H_5^+)^*$ collision complex have different lifetimes (which would imply a dependence on the H_3^+ nuclear spin configuration), or if a subsequent collision with p-H_2 can more effectively stabilize the complex compared with an o-H_2 collision. It is also unclear whether this same effect would occur at higher temperatures, as these ternary association reactions become much slower. Because of this uncertainty, we assume that the rate of H_5^+ formation is independent of the spin configuration of H_3^+, and that the $(H_5^+)^*$ lifetime is independent of its spin configuration.

We instead treat the second of those processes: proton scrambling through $(H_7^+)^*$. A full treatment of this process is difficult, but we make the assumption that a given $(H_5^+)^*$ collision complex will undergo at most one reactive collision with H_2 during its lifetime, and this allows us to use the nuclear spin branching fractions in a similar manner as in the two-body case. The relevant reactions and their rates are listed in Table VIII.

In order to use the nuclear spin branching fractions, the fraction of the $(H_5^+)^*$ complexes that undergo an additional collision with H_2 must be taken into account. First, it is important to note that any "identity" reaction is indistinguishable from a nonreactive collision. Because the two-body and three-body reaction channels may have different identity branching fractions (and different overall rates), we redefine all rates in terms of the rates of reactive collisions: those that result in a hop or exchange process. We will employ subscripts 2 and 3 to refer to two-body ($H_3^+ + H_2$) and three-body [$(H_5^+)^* + H_2$] branching fractions, respectively:

$$S_n^{\mathrm{id}} + S_n^{\mathrm{hop}} + S_n^{\mathrm{exch}} = 1 \ (n = 2, 3),$$
$$k_{3,2}^R = k_{3,2}^L\left(1 - S_2^{\mathrm{id}}\right),$$
$$k_{5,2}^R = k_{5,2}^L\left(1 - S_3^{\mathrm{id}}\right),$$
$$\alpha_n = \frac{S_n^{\mathrm{hop}}}{S_n^{\mathrm{exch}}} = \frac{\Sigma_n^H}{\Sigma_n^E},$$
$$\Sigma_n^H + \Sigma_n^E = 1.$$

The coefficients k^R are the reactive rate coefficients; those with the identity reactions removed. We then define branching fractions Σ_n^M to refer to the branching fractions of only the reactive collisions. The ratio Σ_n^H/Σ_n^E is equal to $S_n^{\mathrm{hop}}/S_n^{\mathrm{exch}}$, so the change in how the overall rate coefficients is defined does not affect the ratio of the hop and exchange rates.

The utility of these redefinitions is that the branching fraction between two-body and three-body processes can now be expressed in terms of a single parameter. Once $(H_5^+)^*$ is formed, the fractions Φ_2 and Φ_3 for the two channels are

$$\Phi_2 = \frac{k_5^u}{k_5^u + k_{5,2}^R[H_2]},$$
$$\Phi_3 = \frac{k_{5,2}^R[H_2]}{k_5^u + k_{5,2}^R[H_2]}, \text{ and consequently}$$
$$\Phi_2 + \Phi_3 = 1.$$

As expected, these show that with increasing $[H_2]$, three-body processes become important, and that the density at which this happens depends on the lifetime of $(H_5^+)^*$ prior to unimolecular dissociation compared to the magnitude of $k_{5,2}^R[H_2]$.

The final step before writing down steady state reaction rates is to calculate the final branching fractions for o-H_3^+ and p-H_3^+ through the three-body process. In Sec. II B, the branching fractions for reactant and product H_5^+ were derived. These must be combined with the branching fractions for the formation of nuclear spin states of $(H_5^+)^*$ through the $H_3^+ + H_2$ collision, as well as the branching fractions for formation of o-H_3^+ and p-H_3^+ resulting from the breakup of nuclear spin states of $(H_5^+)^*$. Using the angular momentum algebra of Oka,[10] this is straightforward.

For the formation of $(H_5^+)^*$, the branching fractions are obtained from the statistical weights of the angular momentum representations resulting from H_3^+ and H_2. We show them as coefficients for emphasis:

$$\mathcal{D}_{3/2} \otimes \mathcal{D}_1 \rightarrow 6(\mathcal{D}_{5/2}/6) \oplus 4(\mathcal{D}_{3/2}/4) \oplus 2(\mathcal{D}_{1/2}/2),$$
$$\mathcal{D}_{3/2} \otimes \mathcal{D}_0 \rightarrow 4(\mathcal{D}_{3/2}/4),$$
$$2\mathcal{D}_{1/2} \otimes \mathcal{D}_1 \rightarrow 8(\mathcal{D}_{3/2}/4) \oplus 4(\mathcal{D}_{1/2}/2),$$
$$2\mathcal{D}_{1/2} \otimes \mathcal{D}_0 \rightarrow 4(\mathcal{D}_{1/2}/2).$$

For the destruction of $(H_5^+)^*$, the statistical weights are

$$\mathcal{D}_{5/2} \rightarrow 6(\mathcal{D}_{3/2} \otimes \mathcal{D}_1/12),$$
$$4\mathcal{D}_{3/2} \rightarrow 4(\mathcal{D}_{3/2} \otimes \mathcal{D}_1/12) \oplus 4(\mathcal{D}_{3/2} \otimes \mathcal{D}_0/4) \oplus 8(\mathcal{D}_{1/2} \otimes \mathcal{D}_1/6),$$
$$5\mathcal{D}_{1/2} \rightarrow 2(\mathcal{D}_{3/2} \otimes \mathcal{D}_1/12) \oplus 4(\mathcal{D}_{1/2} \otimes \mathcal{D}_1/6) \oplus 4(\mathcal{D}_{1/2} \otimes \mathcal{D}_0/2).$$

Keeping in mind that the spin configuration of the product H_2 is unimportant for a pulsed laboratory plasma, the branching fractions for the H_3^+ spin configurations can be obtained. These are listed explicitly in Tables IX and X. To obtain the overall o-H_3^+ and p-H_3^+ branching fractions for a the $H_3^+ + 2H_2$ process, Tables VII, IX, and X can be carefully treated with matrix multiplication. The results are listed in Table XI.

TABLE IX. Branching fractions for the spin configuration of $(H_5^+)^*$ formed in collisions of H_3^+ and H_2.

(H_3^+,H_2)	$\mathcal{D}_{5/2}$	$\mathcal{D}_{3/2}$	$\mathcal{D}_{1/2}$
(o-H_3^+,o-H_2)	3/6	2/6	1/6
(o-H_3^+,p-H_2)	0	1	0
(p-H_3^+,o-H_2)	0	2/3	1/3
(p-H_3^+,p-H_2)	0	0	1

Having calculated these branching fractions, it is now possible to write the equation for $\mathrm{d}/\mathrm{d}t([p\text{-}H_3^+])$. Equation (18) shows the result, having applied the steady state approximation and divided by the product $[H_3^+][H_2]$, as was done in the derivation of the two-body model. Making the substitutions $\Phi_3 = 1 - \Phi_2$, $\Sigma_n^H = \alpha_n/(1+\alpha_n)$, and $\Sigma_n^E = 1/(1+\alpha_n)$, solving for p_3, and simplifying leads to Eq. (19), the high temperature three-body model.

$$
\begin{aligned}
0 = \frac{1}{[H_3^+][H_2]}\frac{\mathrm{d}[p\text{-}H_3^+]}{\mathrm{d}t} = \Phi_2\Bigg(&\left\{\Sigma_2^H\left[\frac{1}{3}(1-p_2)+p_2\right]+\Sigma_2^E\left[\frac{1}{3}(1-p_2)+\frac{1}{3}p_2\right]\right\}(1-p_3)\\
&-\left\{\Sigma_2^H\frac{2}{3}(1-p_2)+\Sigma_2^E\left[\frac{1}{3}(1-p_2)+\frac{1}{3}p_2\right]\right\}p_3\Bigg)\\
+\Phi_3\Bigg(&\Bigg\{\Sigma_3^H\left[\frac{39}{100}(1-p_2)^2+\frac{9}{20}p_2(1-p_2)+\frac{59}{100}(1-p_2)p_2+\frac{13}{20}p_2^2\right]\\
&+\Sigma_3^E\left[\frac{19}{50}(1-p_2)^2+\frac{1}{2}p_2(1-p_2)+\frac{19}{50}(1-p_2)p_2+\frac{1}{2}p_2^2\right]\Bigg\}(1-p_3)\\
&-\Bigg\{\Sigma_3^H\left[\frac{13}{25}(1-p_2)^2+\frac{23}{50}p_2(1-p_2)+\frac{8}{25}(1-p_2)p_2+\frac{13}{50}p_2^2\right]\\
&+\Sigma_3^E\left[\frac{11}{25}(1-p_2)^2+\frac{8}{25}p_2(1-p_2)+\frac{11}{25}(1-p_2)p_2+\frac{8}{25}p_2^2\right]\Bigg\}p_3\Bigg),
\end{aligned}
\tag{18}
$$

$$
p_3 = \frac{\frac{\Phi_2}{1+\alpha_2}\left(\frac{1}{3}\alpha_2+\frac{2}{3}\alpha_2 p_2+\frac{1}{3}\right)+\frac{1-\Phi_2}{1+\alpha_3}\left(\frac{39}{100}\alpha_3+\frac{13}{50}\alpha_3 p_2+\frac{19}{50}+\frac{3}{25}p_2\right)}{\frac{\Phi_2}{1+\alpha_2}\left(\alpha_2+\frac{2}{3}\right)+\frac{1-\Phi_2}{1+\alpha_3}\left(\frac{91}{100}\alpha_3+\frac{41}{50}\right)}. \tag{19}
$$

The results of the model are plotted in Fig. 2. As evident in Eq. (19), when $\Phi_2 = 1$, the three-body terms drop out of the equation and the two-body high temperature model [Eq. (17)] is obtained. This can be seen visually in panels a, b, and c of the figure as the red lines depicting $\Phi_2 = 1$ overlap with the corresponding α_2 value in the two-body model. When $\Phi_2 = 0$, the three-body process exclusively determines p_3, and this is shown in panel d for various values of α_3. When $\alpha_3 = \infty$, the results are identical to the two-body model with $\alpha_2 = 0.5$, and as α_3 decreases, the slope becomes more shallow. Panels a and b show the effects of an increasing effect of three-body reactions where $\alpha_2 = 2.0$, which is close to the value reported by Cordonnier and coworkers.[20] Three-body collisions effectively decrease the slope of the p_3 vs p_2 plot compared to the two-body model with the same α_2. If proton scrambling through the $(H_7^+)^*$ complex is influencing experimental measurements, a fit of the data to the two-body model would provide a lower limit on the value of α_2. Measurement at multiple pressures, however, would eliminate this ambiguity, because if three-body collisions are important, the slope should decrease with increasing pressure (and therefore decreasing Φ_2). Finally, Fig. 2(c) shows the effect of decreasing Φ_2 if both hop/exchange ratios are at their statistical values ($\alpha_2 = 0.5$ and $\alpha_3 = 1.0$).

TABLE X. Branching fractions for the spin configuration of H_3^+ formed upon dissociation of $(H_5^+)^*$.

$(H_5^+)^*$	o-H_3^+	p-H_3^+
$\mathcal{D}_{5/2}$	1	0
$4\mathcal{D}_{3/2}$	1/2	1/2
$5\mathcal{D}_{1/2}$	1/5	4/5

TABLE XI. Mechanism-specific nuclear spin branching fractions for H_3^+ resulting from the three-body reaction $H_3^+ + 2H_2$. Reactant H_2' is the H_2 that collides with $(H_5^+)^*$.

Reactants	Hop		Exchange	
(H_3^+,H_2,H_2')	o-H_3^+	p-H_3^+	o-H_3^+	p-H_3^+
(o-H_3^+,o-H_2,o-H_2')	61/100	39/100	31/50	19/50
(o-H_3^+,o-H_2,p-H_2')	41/100	59/100	31/50	19/50
(o-H_3^+,p-H_2,o-H_2')	11/20	9/20	1/2	1/2
(o-H_3^+,p-H_2,p-H_2')	7/20	13/20	1/2	1/2
(p-H_3^+,o-H_2,o-H_2')	13/25	12/25	11/25	14/25
(p-H_3^+,o-H_2,p-H_2')	8/25	17/25	11/25	14/25
(p-H_3^+,p-H_2,o-H_2')	23/50	27/50	8/25	17/25
(p-H_3^+,p-H_2,p-H_2')	13/50	37/50	8/25	17/25

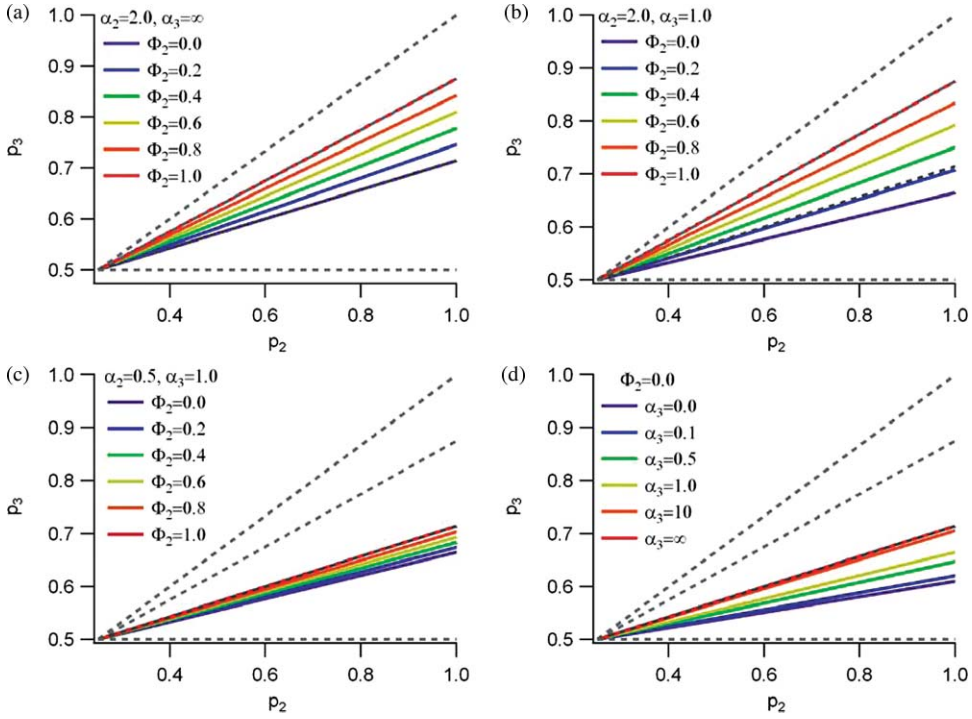

FIG. 2. The three-body high temperature model [Eq. (19)] for various values of Φ_2, α_2, and α_3. For reference, the gray dotted lines are the two-body high temperature model [Eq. (17)] for $\alpha = \{0, 0.5, 2.0, \infty\}$ from shallowest to steepest slope.

It is important to keep in mind that this model is constrained to allow only one three-body scrambling reaction to occur. Therefore, as Φ_2 decreases, the realism of this model might also decrease, as it could be possible for $(H_5^+)^*$ to experience multiple collisions with H_2 prior to dissociation. Also, this model does not treat nuclear spin dependence of the ternary association reaction $H_3^+ + 2H_2 \rightarrow H_5^+ + H_2$, which may have different rates for o-H_3^+ and p-H_3^+. The purpose of the model is to give a sense of what the experimental data may look like if three-body nuclear-spin-dependent processes begin to compete with the $H_3^+ + H_2$ nuclear spin dependence, not to serve as an accurate model for determining the full kinetics of the system.

IV. LOW TEMPERATURE MODEL

At lower temperatures, the assumption that many states are energetically accessible and populated breaks down, and the NSSWs cannot be used to determine the outcomes of many $H_3^+ + H_2$ reactions.[30] It is possible to account for the interplay of nuclear spin selection rules and energetic restrictions by employing a microcanonical statistical approach. Park and Light[23] have developed a microcanonical statistical model for the $H_3^+ + H_2$ system that conserves energy, angular momentum (both motional and nuclear spin), and parity, and also allows for incomplete proton scrambling. The output of their model gives rate coefficients k_{ijkl}, where the subscripts denote the nuclear spin configurations of the reactants and products: i-$H_3^+ + j$-$H_2 \rightarrow k$-$H_3^+ + l$-H_2. The rate coefficients depend on the reactants' total energy (based on their kinetic temperature $T_{\rm kin}$ and rotational temperature $T_{\rm rot}$), as well as the branching fractions $S^{\rm id}$, $S^{\rm hop}$, and $S^{\rm exch}$.

Because the rate coefficients themselves are not broken into identity, hop, and exchange components, another model must be derived. The derivation has been presented in detail elsewhere,[19] but will be summarized here. As with the high temperature models, we assume that the nuclear spin configuration is determined entirely by the $H_3^+ + H_2$ reaction, and ignore formation and destruction of H_3^+. We also ignore three-body processes, and invoke the steady state approximation:

$$\begin{aligned} 0 = \frac{\mathrm{d}[p\text{-}H_3^+]}{\mathrm{d}t} = &\left\{(k_{oopo} + k_{oopp})[o\text{-}H_2]\right. \\ &\left. + (k_{oppo} + k_{oppp})[p\text{-}H_2]\right\}[o\text{-}H_3^+] \\ &- \left\{(k_{pooo} + k_{poop})[o\text{-}H_2]\right. \\ &\left. + (k_{ppoo} + k_{ppop})[p\text{-}H_2]\right\}[p\text{-}H_3^+]. \end{aligned}$$

From the nuclear spin selection rules, k_{oppp} and k_{ppop} are rigorously 0 (see Table I). Dividing through by $[H_3^+][H_2]$ and solving for p_3 gives the final result:

$$p_3 = \frac{(k_{oopp} + k_{oopo})(1 - p_2) + k_{oppo}\,p_2}{(k_{oopp} + k_{oopo} + k_{poop} + k_{pooo})(1 - p_2) + (k_{oppo} + k_{ppoo})p_2}. \tag{20}$$

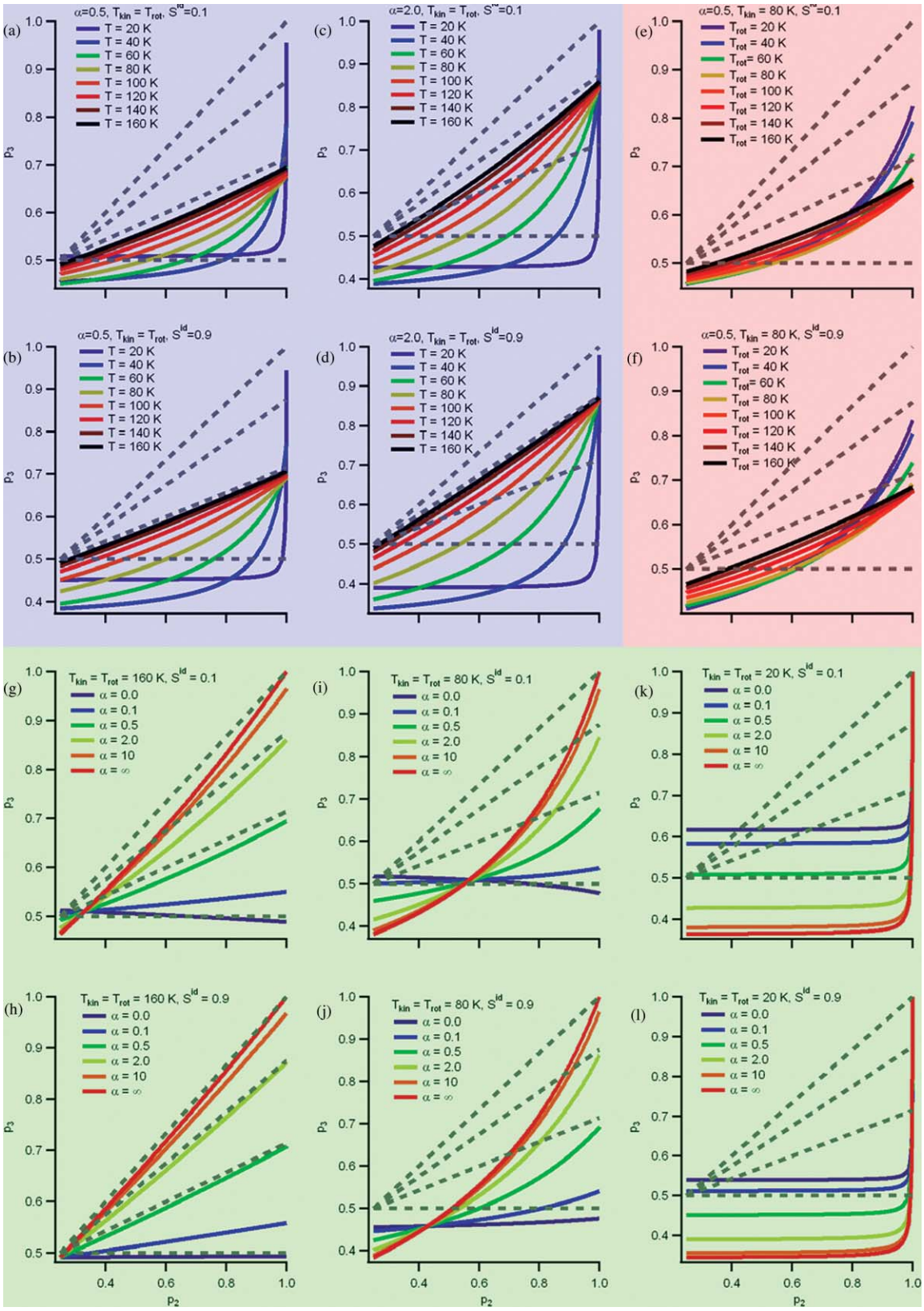

FIG. 3. Low temperature model [Eq. (20)] results for a variety of temperatures and branching fractions. The gray dotted lines are the two-body high temperature model [Eq. (17)] for $\alpha = \{0, 0.5, 2.0, \infty\}$ from shallowest to steepest slope.

Equation (20) is the low temperature model, and it converges to Eq. (17) in the limit that $(k_{oopp} + k_{oopo}) = (k^H + k^E)/3$, $k_{oppo} = k^H + k^E/3$, and so on. This model can be more directly used with the low-temperature (10–160 K) rate coefficients k_{ijkl} calculated by the microcanonical statistical model of Park and Light.[23] This model has been previously applied to the conditions of diffuse molecular clouds in the interstellar medium, and it should be noted that although Eq. (20) is the same as that in Ref. 19, the conditions of a pulsed laboratory plasma are quite different than those in the diffuse molecular clouds. In the latter, the density is so low that the collision timescale (months) is longer than the spontaneous emission timescale (days) for most H_3^+ rotational levels. As a result, essentially all of the H_3^+ population lies in the lowest *ortho* and *para* rotational levels, and consequently the authors calculated rate coefficients at a "nonthermal" rotational temperature of 10 K, and kinetic temperatures from 10 to 160 K. In the laboratory, the collision rate is many orders of magnitude faster than the spontaneous emission rate, and "thermal" rotational temperatures are appropriate.

Results from the low temperature model are plotted in Fig. 3. In general, the model shows that the p_3 vs p_2 traces are curved upwards; the curvature is greater at lower temperatures. As the temperature increases (panels a, b, c, and d; the blue shaded region), the results approach the high temperature model line for the same α. In panels a and b, $\alpha = 0.5$ and $S^{\text{id}} = 0.1$ and 0.9, respectively, and as T approaches 160 K, the curves approach the high temperature model $\alpha = 0.5$ line, especially at higher S^{id}, though it is interesting to note that p_3 is still expected to be less than 0.5 in a n-H_2 plasma. Panels c and d show the same effect for $\alpha = 2.0$. The implications of a nonthermal plasma ($T_{\text{kin}} \neq T_{\text{rot}}$) are shown in panels c and f (the red shaded region; the effect is a subtle change in the curvature, particularly towards larger p_2.

The p_3 vs p_2 traces from the low temperature model are strongly dependent on α, as shown in panels g-l (the green shaded region). Depending on the temperature, the curves could be very close to those of the high temperature model (panels g and h), or dramatically different (panels k and l). Of particular interest are the results at the lowest temperatures. Generally, the differences in the curves due to a large change in S^{id} are subtle. But as seen in the panels k and l, if α is known, then according to this model S^{id} can be determined by the exact value of p_3 across the range of p_2 where the curve is nearly flat.

The low temperature model is only as good as the rate coefficients that are used with it. The rate coefficients used in this work are calculated using the microcanonical statistical model of Park and Light,[23] which is not a quantum mechanical model. If quantum effects become important at low temperatures, then the rate coefficients calculated using a statistical model may not be accurate. However, microcanonical statistical calculations of rate coefficients in other isotopic analogs of the $H_3^+ + H_2$ system have been found to agree well with ion trap measurements at 10–20 K,[31] which provides some support for the use of these rate coefficients in the purely hydrogenic system at similar temperatures. Reactive scattering calculations on the H_5^+ potential energy surface[32] are desirable, but still unfeasible. At more moderate temperatures, it would be unlikely for quantum effects to be important, and it is therefore likely that this model should perform well.

Extension of this model to include three-body scrambling is not straightforward. An analogous microcanonical statistical study of the $H_5^+ + H_2$ reaction would have to be carried out, and the complex formation rates compared with the complex lifetimes to determine the two-body:three-body ratio. Also, the nuclear spin dependence of ternary association reactions would also likely have to be taken into account, as these reactions are much faster at low temperatures. Such work is beyond the scope of this paper, and so the low temperature model that we have derived should only be employed at densities low enough to preclude three-body reactions.

V. CONCLUSIONS

In this paper, we have derived a series of models aimed at extracting the nuclear spin dependence of the $H_3^+ + H_2$ reaction from laboratory data. The appropriate experiment is to measure the p-H_3^+ fraction (p_3) formed in laboratory plasmas of varying p-H_2 fraction (p_2) at steady state. An important condition for using these models is that p_3 must be determined exclusively by the $H_3^+ + H_2$ reaction, not by other nuclear spin dependent processes like electron dissociative recombination of H_3^+. Another important condition is that the p-H_2 fraction is constant, or at the very least, slowly changing, as is the case in the early stages of a pulsed plasma or in a plasma in which the H_2 has an external means of thermalizing its spin.

The nuclear spin dependence of the $H_3^+ + H_2$ reaction is influenced heavily by nuclear spin selection rules that arise as a consequence of exchange symmetry, and can be expressed in terms of the hop-to-exchange ratio α. At sufficiently high temperatures, the nuclear spin selection rules are expected to entirely determine the reaction outcome, and a steady state chemical model incorporating the resultant mechanism-specific product spin branching fractions [Eq. (17)] indicates that α can be determined from the slope of a plot of p_3 vs p_2.

However, in a laboratory plasma, there exists the possibility that the H_2 number density is sufficiently high to allow for three-body collisions to occur, resulting in processes such as ternary association to form H_5^+ or three-body scrambling in the $(H_7^+)^*$ collision complex. In Sec. II B we derived mechanism-specific product spin branching fractions for the $H_5^+ + H_2$ reaction in an analogous manner to the $H_3^+ + H_2$ reaction, using the "H_3^+ hop" and "hydrogen exchange" mechanisms. These branching fractions are incorporated into a steady state kinetic model with the two-body branching fractions [Eq. (19)], where the p_3 vs p_2 plot then depends on the hop-to-exchange ratios for the two-body (α_2) and three-body (α_3) processes, and the relative rates of two-body reactive collisions to three-body reactive collisions. The model makes the assumption that ternary association reactions do not have significant nuclear spin dependence, and that a given $(H_5^+)^*$ complex suffers at most one reactive collision with H_2 during its lifetime.

Finally, we have considered lower temperature plasmas in which there is insufficient energy for the nuclear spin product branching fractions to accurately represent the reaction outcomes. Using rate coefficients calculated with a microcanonical statistical approach, we have developed a low temperature model [Eq. (20)] that predicts the p_3 vs p_2 behavior of the plasma in terms of the identity branching fraction S^{id}, α, and the kinetic and rotational temperatures of the plasma. This model has not been extended to include three-body processes. Fully quantum reactive scattering calculations may be required to accurately represent the behavior of this reaction at the lowest temperatures. It is hoped that these models, together with the appropriate experimental measurements, will allow for determination of the nuclear spin dependence of this important fundamental reaction, and will aid in the use of H_3^+ as a probe of astrophysical conditions.

ACKNOWLEDGMENTS

The authors thank Kisam Park for providing code for calculating the rate coefficients used in our modeling work. This work has been supported by NSF PHY 08-55633.

[1]E. B. Wilson, J. C. Decius, and P. C. Cross, *Molecular Vibrations* (McGraw-Hill, New York, 1955).
[2]D. C. Harris and M. D. Bertolucci, *Symmetry and Spectroscopy: An Introduction to Vibrational and Electronic Spectroscopy* (Oxford University Press, New York, 1978).
[3]R. S. Mulliken, Phys. Rev. **59**, 873 (1941).
[4]J. T. Hougen, J. Chem. Phys. **37**, 1433 (1962).
[5]H. C. Longuet-Higgins, Mol. Phys. **6**, 445 (1963).
[6]P. A. M. Dirac, Proc. R. Soc. London **112**, 661 (1926).
[7]W. Pauli, Z. Phys. **31**, 765 (1925).
[8]B. J. McCall, Ph.D. thesis, University of Chicago, 2001.
[9]M. Quack, Mol. Phys. **34**, 477 (1977).
[10]T. Oka, J. Mol. Spectrosc. **228**, 635 (2004).
[11]P. Drossart, J.-P. Maillard, J. Caldwell, S. J. Kim, J. K.G. Watson, W. A. Majewski, J. Tennyson, S. Miller, S. K. Atreya, J. T. Clarke, J. H. Waite, and R. Wagener, Nature (London) **340**, 539 (1989).
[12]T. R. Geballe, M.-F. Jagod, and T. Oka, Astrophys. J. **408**, L109 (1993).
[13]L. M. Trafton, T. R. Geballe, S. Miller, J. Tennyson, and G. E. Ballester, Astrophys. J. **405**, 761 (1993).
[14]M. Goto, T. Usuda, T. Nagata, T. R. Geballe, B. J. McCall, N. Indriolo, H. Suto, T. Henning, C. P. Morong, and T. Oka, Astrophys. J. **688**, 306 (2008).
[15]B. J. McCall, A. J. Huneycutt, R. J. Saykally, T. R. Geballe, N. Djuric, G. H. Dunn, J. Semaniak, O. Novotny, A. Al-Khalili, A. Ehlerding, F. Hellberg, S. Kalhori, A. Neau, R. Thomas, F. Österdahl, and M. Larsson, Nature (London) **422**, 500 (2003).
[16]N. Indriolo, T. R. Geballe, T. Oka, and B. J. McCall, Astrophys. J. **671**, 1736 (2007).
[17]B. J. McCall, K. H. Hinkle, T. R. Geballe, and T. Oka, Faraday Discuss. **109**, 267 (1998).
[18]E. L. Gibb, S. D. Brittain, T. W. Rettig, M. Troutman, T. Simon, and C. Kulesa, Astrophys. J. **715**, 757 (2010).
[19]K. N. Crabtree, N. Indriolo, H. Kreckel, B. A. Tom, and B. J. McCall, Astrophys. J. **729**, 15 (2011).
[20]M. Cordonnier, D. Uy, R. M. Dickson, K. E. Kerr, Y. Zhang, and T. Oka, J. Chem. Phys. **113**, 3181 (2000).
[21]K. N. Crabtree, C. A. Kauffman, B. A. Tom, E. Beçka, B. A. McGuire, and B. J. McCall, J. Chem. Phys. **134**, 194311 (2011).
[22]D. Gerlich, J. Chem. Soc., Faraday Trans. **89**, 2199 (1993).
[23]K. Park and J. C. Light, J. Chem. Phys. **126**, 044305 (2007).
[24]M. Saporoschenko, Phys. Rev. **139**, A349 (1965).
[25]T. Amano, J. Chem. Phys. **92**, 6492 (1990).
[26]H. Kreckel, M. Motsch, J. Mikosch, J. Glosik, R. Plasil, S. Altevogt, V. Andrianarijaona, H. Buhr, J. Hoffmann, L. Lammich, M. Lestinsky, I. Nevo, S. Novotny, D. A. Orlov, H. B. Pedersen, F. Sprenger, A. S. Terekhov, J. Toker, R. Wester, D. Gerlich, D. Schwalm, A. Wolf, and D. Zajfman, Phys. Rev. Lett. **95**, 263201 (2005).
[27]B. A. Tom, V. Zhaunerchyk, M. B. Wiczer, A. A. Mills, K. N. Crabtree, M. Kaminska, W. D. Geppert, M. Hamberg, M. af Ugglas, E. Vigren, W. J. van der Zande, M. Larsson, R. D. Thomas, and B. J. McCall, J. Chem. Phys. **130**, 031101 (2009).
[28]H. Kreckel, O. Novotný, K. N. Crabtree, H. Buhr, A. Petrignani, B. A. Tom, R. D. Thomas, M. H. Berg, D. Bing, M. Grieser, C. Krantz, M. Lestinsky, M. B. Mendes, C. Nordhorn, R. Repnow, J. Stützel, A. Wolf, and B. J. McCall, Phys. Rev. A **82**, 042715 (2010).
[29]W. Paul, B. Lücke, S. Schlemmer, and D. Gerlich, Int. J. Mass Spectrom. Ion Proc. **149–150**, 373 (1995).
[30]D. Gerlich, F. Windisch, P. Hlavenka, R. Plasīl, and J. Glosik, Phil. Trans. R. Soc. A **364**, 3007 (2006).
[31]E. Hugo, O. Asvany, and S. Schlemmer, J. Chem. Phys. **130**, 164302 (2009).
[32]Z. Xie, B. J. Braams, and J. M. Bowman, J. Chem. Phys. **122**, 224307 (2005).